

NACA RM E57J22

FACILITY FORM 802

N65-12710

(ACCESSION NUMBER)

(THRU)

23

(PAGES)

01

(CATEGORY)

(NASA CR OR TMX OR AD NUMBER)

X 62. 64574

Copy 93
RM E57J22

GPO PRICE \$ _____

OTS PRICE(S) \$ _____

Hard copy (HC) 1.00

Microfiche (MF) .50

NACA

RESEARCH MEMORANDUM

EXPERIMENTAL INVESTIGATION OF A HIGH SUBSONIC MACH
NUMBER TURBINE HAVING A 40-BLADE ROTOR WITH
ZERO SUCTION-SURFACE DIFFUSION

By William J. Nusbaum, Charles A. Wasserbauer, and Cavour H. Hauser

Lewis Flight Propulsion Laboratory
Cleveland, Ohio

DECLASSIFIED - EFFECTIVE 1-15-64

Authority: Memo Geo. Drobka NASA HQ.

Code ATSS-A Dtd. 3-12-64 Subj: Change

in Security Classification Marking.

DOWNGRADED AT 12 YEAR
INTERVALS; NOT AUTOMATICALLY
DECLASSIFIED. DOD DIR 5200.10



NATIONAL ADVISORY COMMITTEE
FOR AERONAUTICS

WASHINGTON

January 16, 1958



T58-1633

5785

DECLASSIFIED



NATIONAL ADVISORY COMMITTEE FOR AERONAUTICS

RESEARCH MEMORANDUM

EXPERIMENTAL INVESTIGATION OF A HIGH SUBSONIC MACH NUMBER

TURBINE HAVING A 40-BLADE ROTOR WITH ZERO

SUCTION-SURFACE DIFFUSION

By William J. Nusbaum, Charles A. Wasserbauer, and
Cavour H. Hauser

DECLASSIFIED - EFFECTIVE 1-15-64
Authority: Memo Geo. Drobka NASA HQ.
Code ATSS-A Dtd. 3-12-64 Subj: Change
in Security Classification Marking.

SUMMARY

12710

An experimental turbine was designed for a high weight flow per unit frontal area, a high specific work output, a relative critical velocity ratio of 0.82 at the rotor hub inlet, and zero rotor blade suction-surface diffusion. At the equivalent design blade speed and work output, the brake internal efficiency based on the actual over-all total-pressure ratio was 0.899. This value is 0.028 greater than the efficiency of a turbine with the same velocity diagrams and approximately the same solidity but with high rotor blade suction-surface diffusion.

The calculated value of the ratio of effective rotor blade momentum thickness to mean camber length of 0.0103 is in very good agreement with the values previously obtained for transonic turbines having the same average total surface diffusion parameter. This value is much smaller than that obtained from a turbine having the same velocity diagrams but with high rotor blade suction-surface diffusion. These results indicate that low suction-surface diffusion is essential for minimum over-all losses through a turbine-rotor blade row.

INTRODUCTION

A research program is in progress at the NACA Lewis laboratory to establish values of design parameters that will result in a turbine with high efficiency, high mass flow per unit frontal area, and high specific work output per stage. In order to achieve these goals a value of solidity for the rotor blade row should be selected that will give minimum over-all rotor losses. A decrease in solidity has the advantage of a reduction in the sum of blade and end-wall surface areas where the boundary layer is produced. However, as the solidity of a blade row is decreased, there is an increase in blade loading with a resultant increase in momentum loss



4676

CO-1

per unit surface area (ref. 1). For low-reaction blade rows an increase in blade loading results in increased values of the total blade surface diffusion parameter, which is equal to the sum of the suction- and pressure-surface diffusion parameters. (The diffusion parameter is defined in the following section, SYMBOLS.) This added diffusion may occur on either the suction or pressure surfaces. Therefore, in order to establish values of design parameters that will result in minimum over-all blade loss, it is necessary to establish the variation of over-all blade loss with solidity, pressure-surface diffusion, and suction-surface diffusion.

The variation of rotor blade boundary-layer momentum-thickness parameter $\bar{\theta}_{tot}/l$ with diffusion parameter for five transonic turbine designs is presented in reference 2. These turbines, designed for high work output, have a relative inlet critical velocity ratio of unity at the hub of the rotor.

In order to obtain additional information on the effect of solidity and blade surface diffusion on over-all blade loss, a program was initiated to obtain the over-all performance of a series of high subsonic Mach number turbines having high weight flow per unit frontal area and high specific work output. All the turbine configurations of this series have the same velocity diagrams. The rotor hub inlet relative critical velocity ratio is 0.82. The same stator was used throughout the investigation. The rotors have the same value of radial tip clearance (0.030 in.). The apparatus, instrumentation, and test procedure were the same for all the turbines of the series. The only parameters that were allowed to vary were the rotor blade solidity and the surface velocity distribution on the rotor blades which determine the value of blade surface diffusion.

The design and over-all performance of the first turbine of the series are presented in reference 3. The rotor of this turbine, hereinafter referred to as configuration I, had 58 blades with relatively low diffusion on the blade surfaces.

The over-all performance of the second of this series of high subsonic Mach number turbines, hereinafter referred to as configuration II, is presented in reference 4. The rotor of this turbine had 40 blades with a considerably higher value of suction-surface diffusion than that of configuration I.

The subject investigation evaluates the over-all performance of configuration III, which has 40 rotor blades and therefore approximately the same solidity as configuration II but with zero diffusion on the rotor blade suction surface. The results of the performance investigation at equivalent design conditions are also evaluated in terms of the ratio of effective rotor blade momentum thickness to mean camber length $\bar{\theta}_{tot}/l$

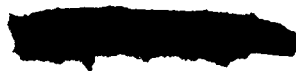
and are compared with the values for the five transonic turbine rotors of reference 2 and with the values for the rotors of configurations I and II (refs. 3 and 4).

SYMBOLS

A_f	turbine tip frontal area, sq ft
a_{cr}	critical velocity of sound, ft/sec
D_p	pressure-surface diffusion parameter, $\frac{\text{Blade-inlet relative velocity} - \text{Min. blade surface relative velocity}}{\text{Blade-inlet relative velocity}}$
D_s	suction-surface diffusion parameter, $\frac{\text{Max. blade surface relative velocity} - \text{Blade-outlet relative velocity}}{\text{Max. blade surface relative velocity}}$
D_{tot}	sum of suction- and pressure-surface diffusion parameters, $D_p + D_s$
$\Delta h'$	specific work output, Btu/lb
l	length of mean camber line, ft
p	absolute pressure, lb/sq ft
r	radius, ft
U	blade velocity, ft/sec
V	absolute gas velocity, ft/sec
W	relative gas velocity, ft/sec
w	weight flow, lb/sec
β	relative gas-flow angle measured from axial direction, deg
γ	ratio of specific heats
γ^0	blade-chord angle, angle between blade chord and axial direction, deg
δ	ratio of inlet air total pressure to NACA standard sea-level pressure, p_1'/p^*

4676

CO-1 beck



ϵ function of $\gamma, \frac{\gamma^*}{\gamma} \left[\frac{\frac{\gamma}{\gamma-1} \left(\frac{\gamma+1}{2} \right)}{\frac{\gamma^*}{\gamma^*-1} \left(\frac{\gamma^*+1}{2} \right)} \right]$

η brake internal efficiency, defined as ratio of turbine work (based on torque, weight flow, and speed measurements) to ideal work (based on inlet total temperature and inlet and outlet total pressures, both defined as sum of static pressure and pressure corresponding to gas velocity)

η_x brake internal rating efficiency, defined as ratio of turbine work (based on torque, weight flow, and speed measurements) to ideal work (based on inlet total temperature and inlet and outlet total pressures, both defined as sum of static pressure and pressure corresponding to axial component of velocity)

θ_{cr} squared ratio of critical velocity at turbine inlet to critical velocity at NACA standard sea-level temperature, $(a'_{cr,1}/a^*_{cr})^2$

$\bar{\theta}_{tot}$ effective rotor blade momentum thickness based on turbine over-all performance, ft

Subscripts:

- h hub
- m mean
- t tip
- u tangential
- x axial
- 1 station upstream of stator
- 2 station at trailing edge of stator
- 3 station at free-stream condition between stator and rotor
- 4 station at trailing edge of rotor
- 5 station downstream of rotor

Superscripts:

- * NACA standard condition
- ' stagnation state
- " relative stagnation state

TURBINE DESIGN

Design Requirements

The design requirements of the subject turbine, which are the same as those for all the turbines of this series, are included herein for convenience:

Equivalent specific work output, $\Delta h' / \omega_{cr}$, Btu/lb	20.60
Equivalent specific weight flow, $\epsilon w \sqrt{\omega_{cr}} / \delta A_f$, (lb/sec)/sq ft . . .	15.06
Equivalent blade tip speed, $U_t / \sqrt{\omega_{cr}}$, ft/sec	720

The velocity diagrams for the subject turbine and configuration II are identical and are shown in figure 1. Configuration I has the same free-stream velocity diagrams but has a slightly different velocity in the plane of the trailing edge (station 4) because of a small difference in blockage.

The rotor of the subject turbine was designed with the same number of blades and approximately the same solidity as that of configuration II but with zero diffusion on the suction surface. It was assumed that simplified radial equilibrium exists along radial elements through the midchannel streamline at each axial station through the blade passage. The total-pressure drop between stations 3 and 4 was assumed to occur linearly in the axial direction.

Procedure

In general, the three-dimensional blade design procedure of reference 5 was used. The following steps summarize this procedure:

- (1) A blade shape was first approximated.
 - (a) For the hub, mean, and tip radial stations a straight suction surface was drawn from the throat to the trailing edge at angles $\beta_{4,h}$, $\beta_{4,m}$, and $\beta_{4,t}$, respectively.

- (b) At each radial station a straight suction surface from the leading edge to the potential line at the channel inlet was drawn at an angle equal to or slightly less than the flow inlet angle β_3 .
- (c) The channel was then drawn such that a reasonable blade shape resulted.
- (2) In order to obtain a reasonable hub midchannel velocity distribution as a first trial, a constant velocity equal to the blade-outlet velocity was assumed on the suction surface within the guided channel, and the method of appendix B of reference 5 was applied.
- (3) By using the midchannel velocity distribution at the hub and the radial equilibrium relation of appendix B of reference 5, the blade shape was analyzed to obtain the midchannel and surface velocity distributions at the hub, mean, and tip sections.
- (4) With the blade surface velocities determined at the three sections, the weight flow was calculated at each axial station using the method given in reference 6.
- (5) If the results of step (4) indicated that the blade would not pass the design weight flow at any axial station, the midchannel velocity distribution at the hub was altered, and steps (3) and (4) were repeated until the calculated value of weight flow was within 1 percent of the design value.
- (6) If there was an appreciable amount of suction-surface diffusion at any section, the blade shape was altered, a new midchannel velocity distribution was assumed, and steps (3) to (5) were repeated until a final satisfactory blade was evolved.

The resulting blade-section profiles obtained from these steps are shown in figure 2, and the coordinates are given in table I.

In order to obtain the final blade shape the blade profiles for the hub, mean, and tip sections were stacked so that the midpoints of the potential lines across the channel exits at the three sections were on a radial line. A photograph of the rotor is shown in figure 3.

Comparison of Subject Turbine with Configurations I and II

The design midchannel and blade surface velocity distributions for the hub, mean, and tip sections as obtained from the previous procedure are shown in figure 4. The number of blades and the values of the surface

diffusion parameters and solidity for the three configurations are given in table II. Very low values of suction-surface diffusion have been obtained with diffusion parameters D_s equal to 0.02, 0.07, and 0.03 at the hub, mean, and tip sections, respectively. Thus, the subject turbine has an average value of rotor blade suction-surface diffusion equal to 0.04, which is much lower than the value of 0.24 for the rotor of configuration II and is considered negligible in this report. On the pressure surface, however, the subject turbine has an average value of 0.42 as compared with a value of 0.15 for the rotor of configuration II. The resulting average value of the total diffusion parameter is 0.46 as compared with a value of 0.39 for the rotor of configuration II.

In order to obtain low suction-surface diffusion it is generally necessary to design the blades with a long, thin profile downstream of the midchord position. A comparison of the blade profile of the subject turbine with that of configuration II (ref. 4) shows that the subject turbine rotor blades are considerably thinner, particularly near the blade trailing edge. This may be undesirable from a mechanical design standpoint in an actual turbine.

The solidities (based on blade chord) at the hub, mean, and tip sections of the subject turbine rotor are 1.9, 1.7, and 1.6, respectively. The turbine rotor of configuration II has solidities at the hub, mean, and tip sections of 2.1, 1.8, and 1.8, respectively. Thus, the subject turbine rotor has a slightly lower value of solidity, a slightly higher value of total diffusion, and a much lower value of suction-surface diffusion than the turbine rotor of configuration II.

A comparison of the subject 40-blade turbine rotor with the 58-blade rotor of configuration I shows that the average values of suction-surface diffusion for the two rotors are nearly equal. The rotor of configuration I has a pressure-surface diffusion parameter equal to 0.15 as compared with the much larger value of 0.42 for the subject turbine rotor. As a result, the value of the total diffusion parameter for the subject turbine rotor (0.46) is much larger than the value for the rotor of configuration I (0.21).

APPARATUS, INSTRUMENTATION, AND TEST PROCEDURE

For the subject turbine the apparatus, instrumentation, and test procedure are the same as those described in reference 3. The over-all performance data were taken at nominal values of total-pressure ratio p_1/p_5 from 1.3 to the maximum obtainable (about 2.3), while the wheel speed was varied in 5-percent intervals from 60 to 110 percent of equivalent design speed. The absolute inlet total pressure was set at 50 inches of mercury (24.6 lb/sq in. abs), and the inlet total temperature was about 70° F.

RESULTS AND DISCUSSION

Comparison of Over-all Performance of Subject Turbine
with That of Configurations I and II

The over-all performance map for the subject turbine, based on the actual over-all total-pressure ratio p_1'/p_5' , is presented in figure 5(a). The equivalent specific work $\Delta h'/\Theta_{cr}$ is plotted against the weight flow - mean blade speed parameter $\varepsilon w U_m/\delta$ with the actual over-all total-pressure ratio, percent design blade speed, and the brake internal efficiency as parameters. The maximum efficiency, which is also the efficiency at the point of equivalent design specific work and blade speed, is 0.899. This value is 0.028 greater than the efficiency for configuration II at design point and 0.024 greater than the efficiency for configuration I at the same point. Efficiencies of 0.89 or greater are obtained over a large range of operating conditions around design point for total-pressure ratios greater than 1.8 and the percent equivalent design speed greater than 0.90. The efficiency is greater than 0.87 over a large portion of the map.

The turbine performance is also rated by a performance map based on the rating over-all total-pressure ratio $p_1'/p_{5,x}'$ as presented in figure 5(b). The rating efficiency at the point of equivalent design specific work output and blade speed is 0.891. Thus, 0.008 in turbine efficiency was lost in the energy of the exit whirl velocity component $V_{u,5}$.

An indication of the differences in efficiency between the subject turbine and the turbines of configurations I and II at the point of equivalent design specific work and blade speed can be found by an examination of the velocities downstream of the stator and rotor blades (stations 3 and 5). The variation of the static pressure at these stations with the actual over-all total-pressure ratio at equivalent design blade speed is presented in figure 6. At station 5, downstream of the rotor, the average of hub and tip values of static pressure is presented because there is little variation in static pressure over the blade height. A static-pressure rise occurs across the rotor hub from stations 3 to 5 for total-pressure ratios up to about 2.16, at which point the rotor blades are choked.

Also shown in figure 6 are the measured values of static- to inlet total-pressure ratios at the points of equivalent design specific work for the subject turbine, configuration I, and configuration II. At the points of equivalent design specific work at both stations 3 and 5, the values of the ratio of static pressure to inlet total pressure p/p_1' for the subject turbine are slightly greater than those for configurations I and II. Since all the turbines of the series used the same stator and

operated at the same inlet conditions, the static-pressure measurements indicate that at the points of equivalent design specific work the rotor-inlet tangential velocity component $V_{u,3}$ is slightly less for the subject turbine than for the turbines of configurations I and II. Figure 6 also indicates that, at the rotor exit and at the same points of equivalent design specific work, the ratio of static pressure to total pressure

$$\left(\frac{p}{p'}\right)_5 = \frac{p_5}{p_1} \frac{p_1^i}{p_5^i}$$

for the subject turbine (0.73) is slightly greater than for the turbines of configurations I and II (0.72). Thus, the subject turbine rotor has a slightly lower value of exit velocity V_5 as well as a lower value of the rotor-inlet tangential velocity component $V_{u,3}$. For the same design work output and blade speed the exit relative flow angle and thus the amount of turning must be greater for the subject turbine rotor. In fact, a radial survey of the flow angle at the rotor exit at the point of equivalent design specific work indicates the amount of turning for the subject turbine rotor to be about 3.0° greater than that for the rotor of configuration I and about 5.0° greater than that for the rotor of configuration II. It follows that the losses through the rotor blade row are less for the subject turbine than for the turbines of configurations I and II.

As stated in a previous section, the subject rotor and the rotor of configuration II have the same value of radial tip clearance and the same number of blades. Therefore, it is assumed that they have approximately equal values of tip clearance losses. These two rotors differ mainly in the amount of rotor blade average suction-surface diffusion. Thus, the lower value of rotor blade losses for the subject turbine, as compared with that for the turbine of configuration II, is attributed to a much smaller value of average suction-surface diffusion.

Suction-surface diffusion usually occurs along the part of the blade toward the trailing edge where a boundary layer has developed. The combined effect of a decelerating flow and a thick boundary layer is conducive to flow separation and the resultant blade losses. Pressure-surface diffusion usually occurs along the part of the blade near the leading edge where the boundary layer is thin (see fig. 4). Thus, there is less chance for flow separation to occur on a blade with pressure-surface diffusion than on one with suction-surface diffusion. Even if there is flow separation on the pressure surface, it is very probable that the flow will reattach to the blade surface because of the accelerating flow along the part of the blade toward the trailing edge.

The difference in losses through the rotor blade row between the subject turbine and the turbine of configuration I is probably caused by

the difference in solidity. These two turbines have approximately equal values of rotor blade suction-surface diffusion. However, the rotor of configuration I has a considerably larger value of solidity and, therefore, a greater rotor blade surface area over which boundary-layer losses are developed (ref. 1).

Comparison of Rotor Blade Momentum Thickness of Subject

Turbine with That of Configurations I and II

The ratio of effective rotor blade momentum thickness to mean camber length $\bar{\theta}_{tot}/l$ for the subject turbine was calculated by the method of reference 2. This calculated value of 0.0104 was then corrected for Reynolds number by assuming the momentum thickness inversely proportional to the one-fifth power of the Reynolds number and using the Reynolds number for the transonic turbines (620,000) as a reference value. The corrected value of 0.0103 is plotted against the average design total diffusion parameter of 0.46 in figure 7. This figure also presents the data for the six transonic turbines of reference 2 and for the turbines of configurations I and II. Although it has been stated that suction-surface diffusion appears to be a more important parameter in determining blade losses than pressure-surface diffusion, the latter is also a contributing factor. Therefore, it is to be noted that the blade loss parameter is plotted against the sum of the pressure- and suction-surface parameters in figure 7. The data for the subject turbine show very good agreement with those for the six transonic turbines.

A comparison of the subject turbine with the turbine of configuration II shows that the subject turbine has a smaller value of the loss parameter $\bar{\theta}_{tot}/l$ even though the value of the total surface diffusion parameter for the subject turbine is slightly larger. As stated previously, this difference in blade loss is attributed to a much smaller value of average suction-surface diffusion for the subject turbine rotor as compared with the value for the rotor of configuration II. A similar effect of suction-surface diffusion on blade loss was obtained in the investigation of the transonic turbines (ref. 7).

The value of the loss parameter for the subject turbine rotor is approximately equal to that for the turbine rotor of configuration I. These two rotors have nearly equal values of suction-surface diffusion but differ considerably in solidity and total diffusion. However, the effect of solidity is minimized in the calculation of the loss parameter $\bar{\theta}_{tot}/l$ (ref. 2). Apparently, this loss parameter is not affected greatly by changes in the values of pressure-surface diffusion if the resulting values of total surface diffusion are within the limits represented by these two rotors.

SUMMARY OF RESULTS

The over-all performance of a high subsonic Mach number turbine with comparatively low solidity and zero suction-surface diffusion is presented. The results of the investigation are compared with previously obtained results for transonic turbines and for turbines that have the same velocity diagrams but different values of rotor blade suction-surface diffusion.

The brake internal efficiency based on the actual total-pressure ratio at the equivalent design blade speed and specific work output was 0.899. This value is 0.028 greater than that obtained from a turbine having the same velocity diagrams and approximately the same solidity but with high rotor blade suction-surface diffusion; it is also 0.024 greater than the design-point efficiency obtained from a turbine having the same velocity diagrams and approximately the same value of suction-surface diffusion but having a larger value of solidity. The efficiency based on the rating total-pressure ratio at equivalent design blade speed and specific work output was 0.891.

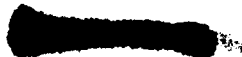
The calculated value of the ratio of effective rotor blade momentum thickness to mean camber length of 0.0103 is in very good agreement with the values previously obtained for transonic turbines. This value is much smaller than that obtained from a turbine having the same velocity diagrams and approximately the same solidity but with a larger value of rotor blade suction-surface diffusion. It is approximately equal to that obtained from a turbine having the same velocity diagrams and about equal values of suction-surface diffusion but having a larger value of solidity.

These results indicate that low suction-surface diffusion is desirable for minimum over-all losses through a turbine rotor blade row. However, in order to obtain low suction-surface diffusion it is generally necessary to design the blades with a long, thin profile downstream of the midchord position, which may be undesirable from a mechanical design standpoint in an actual turbine.

Lewis Flight Propulsion Laboratory
 National Advisory Committee for Aeronautics
 Cleveland, Ohio, October 24, 1957

REFERENCES

1. Miser, James W., Stewart, Warner L., and Whitney, Warren J.: Analysis of Turbomachine Viscous Losses Affected by Changes in Blade Geometry. NACA RM E56F21, 1956.



4676

CO-2 back

2. Stewart, Warner L., Whitney, Warren J., and Miser, James W.: Use of Effective Momentum Thickness in Describing Turbine Rotor-Blade Losses. NACA RM E56B29, 1956.
3. Hauser, Cavour H., and Nusbaum, William J.: Experimental Investigation of a High Subsonic Mach Number Turbine Having Low Rotor Suction-Surface Diffusion. NACA RM E56G25, 1956.
4. Nusbaum, William J., and Hauser, Cavour H.: Experimental Investigation of a High Subsonic Mach Number Turbine Having High Rotor Blade Suction-Surface Diffusion. NACA RM E56I18, 1956.
5. Stewart, Warner L., Wong, Robert Y., and Evans, David G.: Design and Experimental Investigation of Transonic Turbine with Slight Negative Reaction Across Rotor Hub. NACA RM E53L29a, 1954.
6. Miser, James W., Stewart, Warner L., and Monroe, Daniel E.: Effect of High Rotor Pressure-Surface Diffusion on Performance of a Transonic Turbine. NACA RM E55H29a, 1955.
7. Whitney, Warren J., Monroe, Daniel E., and Wong, Robert Y.: Investigation of Transonic Turbine Designed for Zero Diffusion of Suction-Surface Velocity. NACA RM E54F23, 1954.

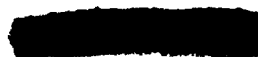
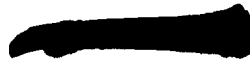
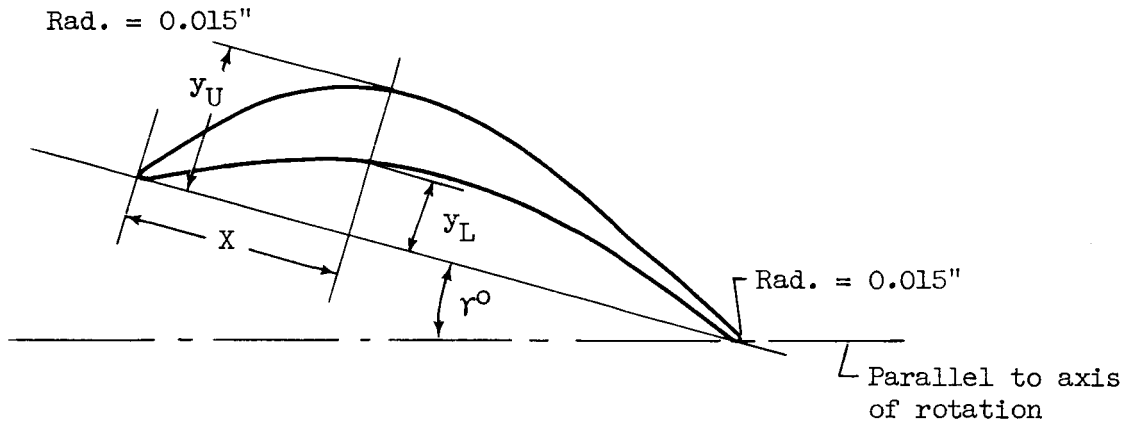


TABLE I. - ROTOR BLADE-SECTION COORDINATES



X, in.	Hub		Mean		Tip	
	$\gamma^0 = 0^\circ$		$\gamma^0 = 22.8^\circ$		$\gamma^0 = 38.2^\circ$	
	$r/r_t = 0.60$		$r/r_t = 0.80$		$r/r_t = 1.00$	
	$y_L,$ in.	$y_U,$ in.	$y_L,$ in.	$y_U,$ in.	$y_L,$ in.	$y_U,$ in.
0	0.015	0.015	0.015	0.015	0.015	0.015
.1	.070	.162	.055	.138	.027	.079
.2	.146	.286	.109	.227	.053	.129
.3	.204	.375	.147	.283	.072	.167
.4	.245	.430	.172	.313	.087	.193
.5	.270	.455	.184	.320	.097	.207
.6	.279	.453	.189	.314	.102	.212
.7	.273	.424	.185	.295	.108	.208
.8	.254	.375	.173	.264	.108	.197
.9	.220	.308	.157	.228	.101	.182
1.0	.174	.234	.135	.191	.096	.165
1.1	.115	.159	.110	.155	.088	.147
1.2	.046	.084	.081	.118	.080	.128
1.28	.015	.015	-----	-----	-----	-----
1.3	-----	-----	.048	.082	.069	.111
1.4	-----	-----	.013	.045	.057	.093
1.453	-----	-----	.015	.015	-----	-----
1.5	-----	-----	-----	-----	.043	.075
1.6	-----	-----	-----	-----	.027	.057
1.7	-----	-----	-----	-----	.010	.040
1.769	-----	-----	-----	-----	.015	.015

TABLE II. - COMPARISON OF ROTOR DESIGN PARAMETERS FOR SUBJECT TURBINE
WITH THOSE FOR TURBINES OF REFERENCES 3 AND 4

Turbine	Section	Rotor blade surface diffusion parameter				
		Suction surface, D_s	Pressure surface, D_p	Total, D_{tot}	Solidity	Number of blades
Configuration I (ref. 3)	Hub	0.00	0.27	0.27	2.8	58
	Mean	.06	.12	.18	2.2	
	Tip	.12	.06	.18	2.0	
	Average	.06	.15	.21		
Configuration II (ref. 4)	Hub	0.31	0.25	0.56	2.1	40
	Mean	.27	.07	.34	1.8	
	Tip	.15	.13	.28	1.8	
	Average	.24	.15	.39		
Configuration III (subject)	Hub	0.02	0.59	0.61	1.9	40
	Mean	.07	.50	.58	1.7	
	Tip	.03	.16	.19	1.6	
	Average	.04	.42	.46		



46/6

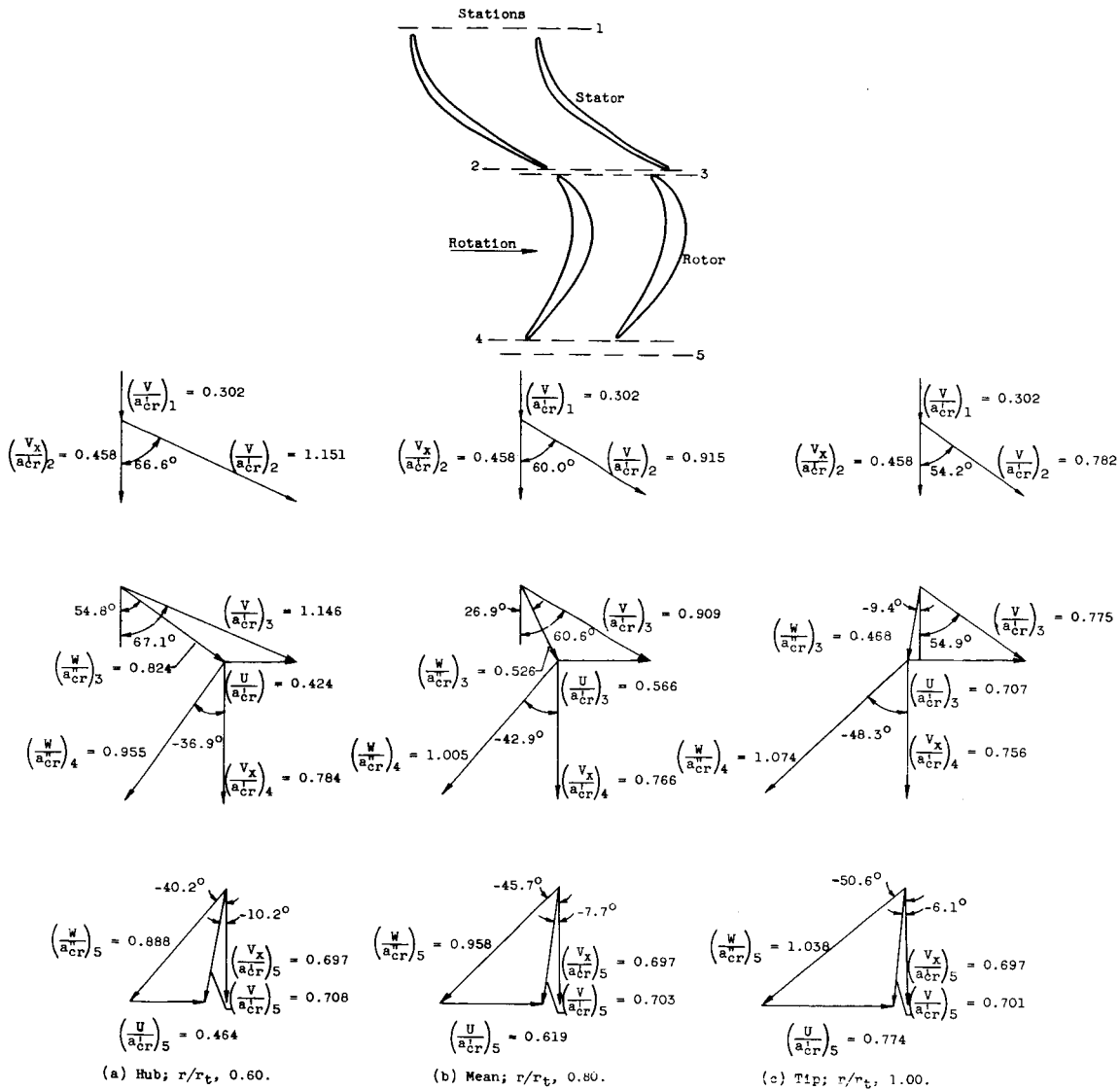
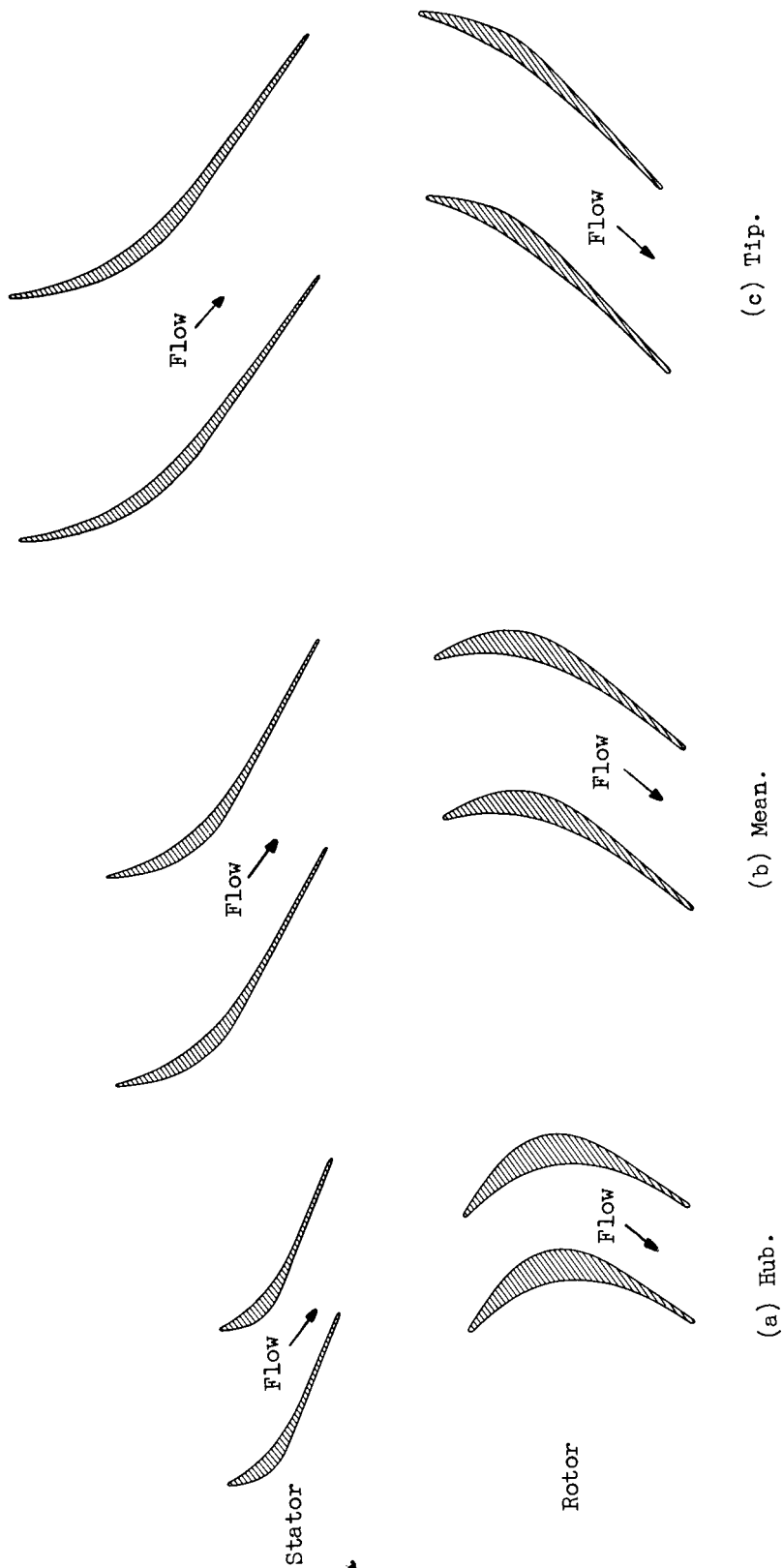


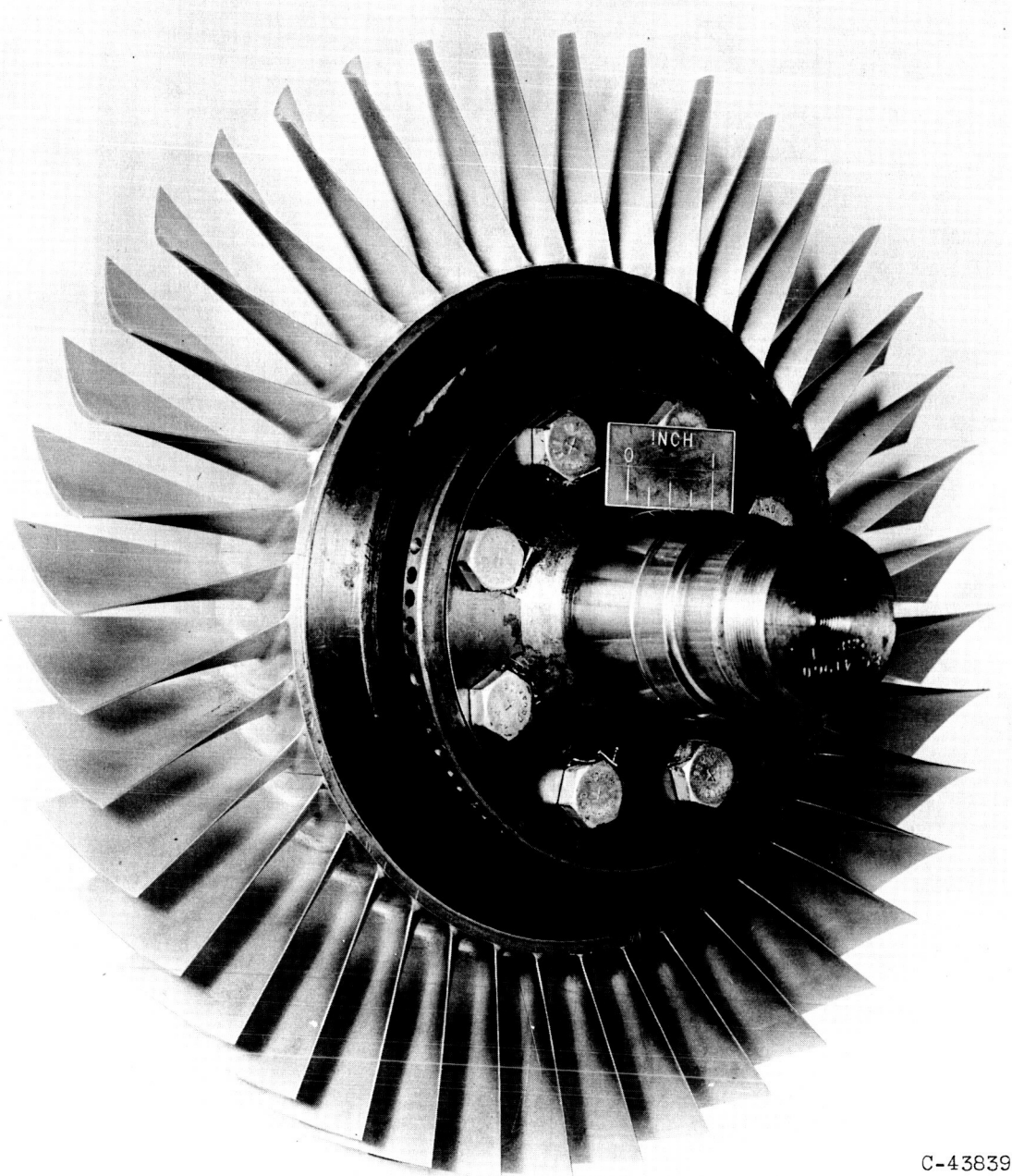
Figure 1. - Velocity diagrams for subject turbine (same as those of configuration II (ref. 4)).





CD-5620

Figure 2. - Stator and rotor blade passages and profiles.



C-43839

Figure 3. - Subject turbine rotor.

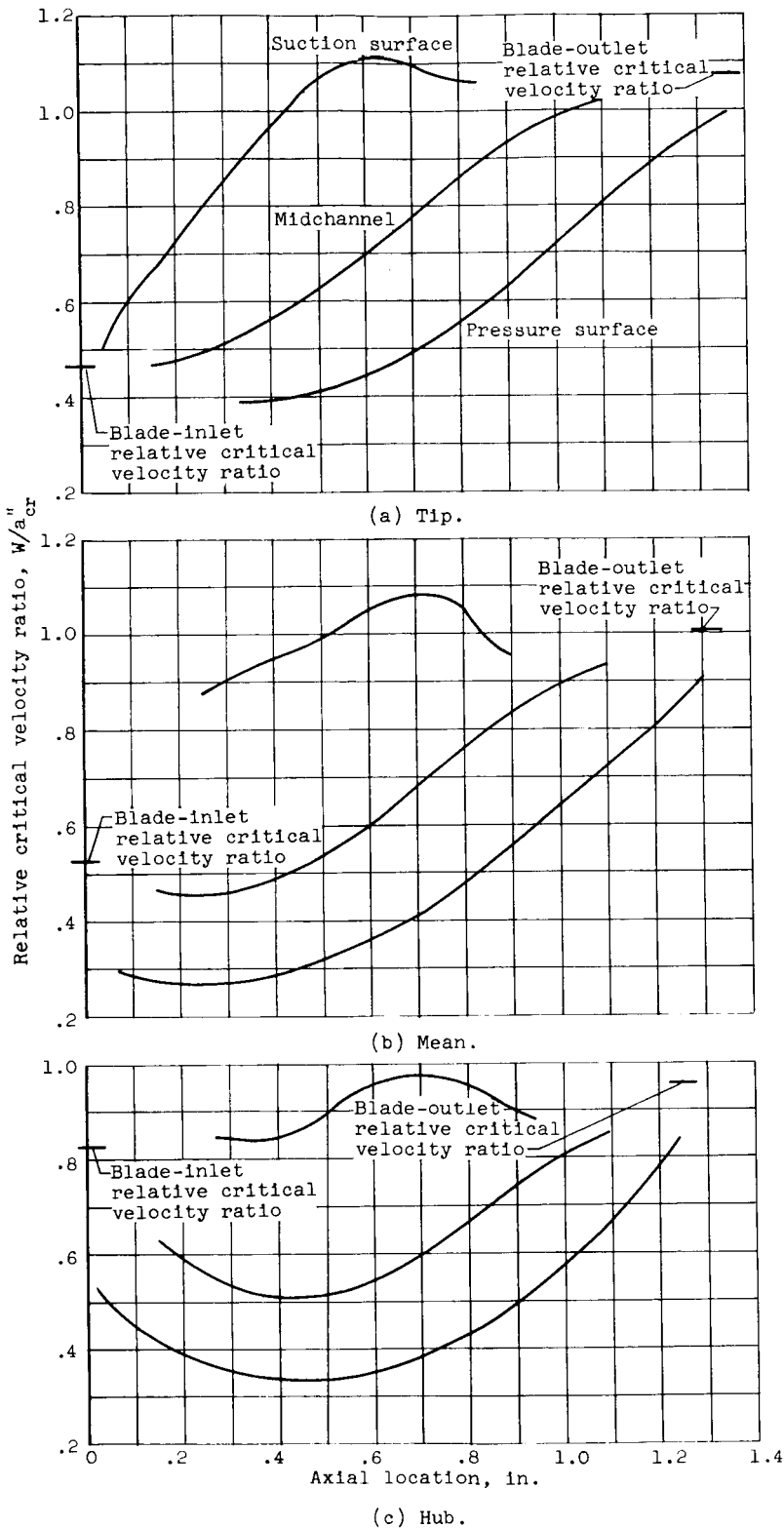
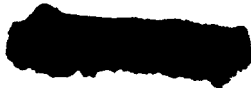
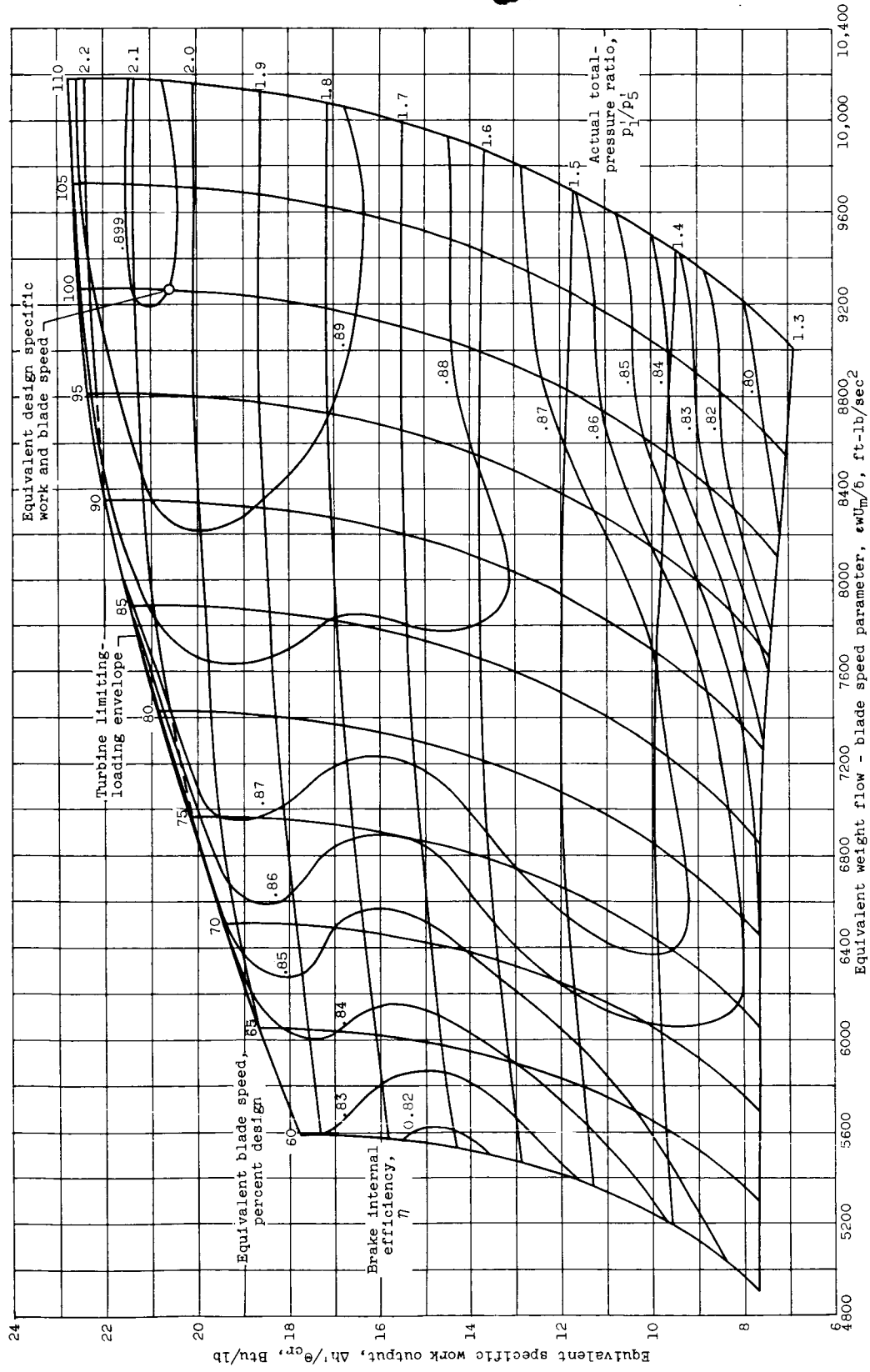


Figure 4. - Design rotor blade midchannel and surface velocity distribution at hub, mean, and tip sections.

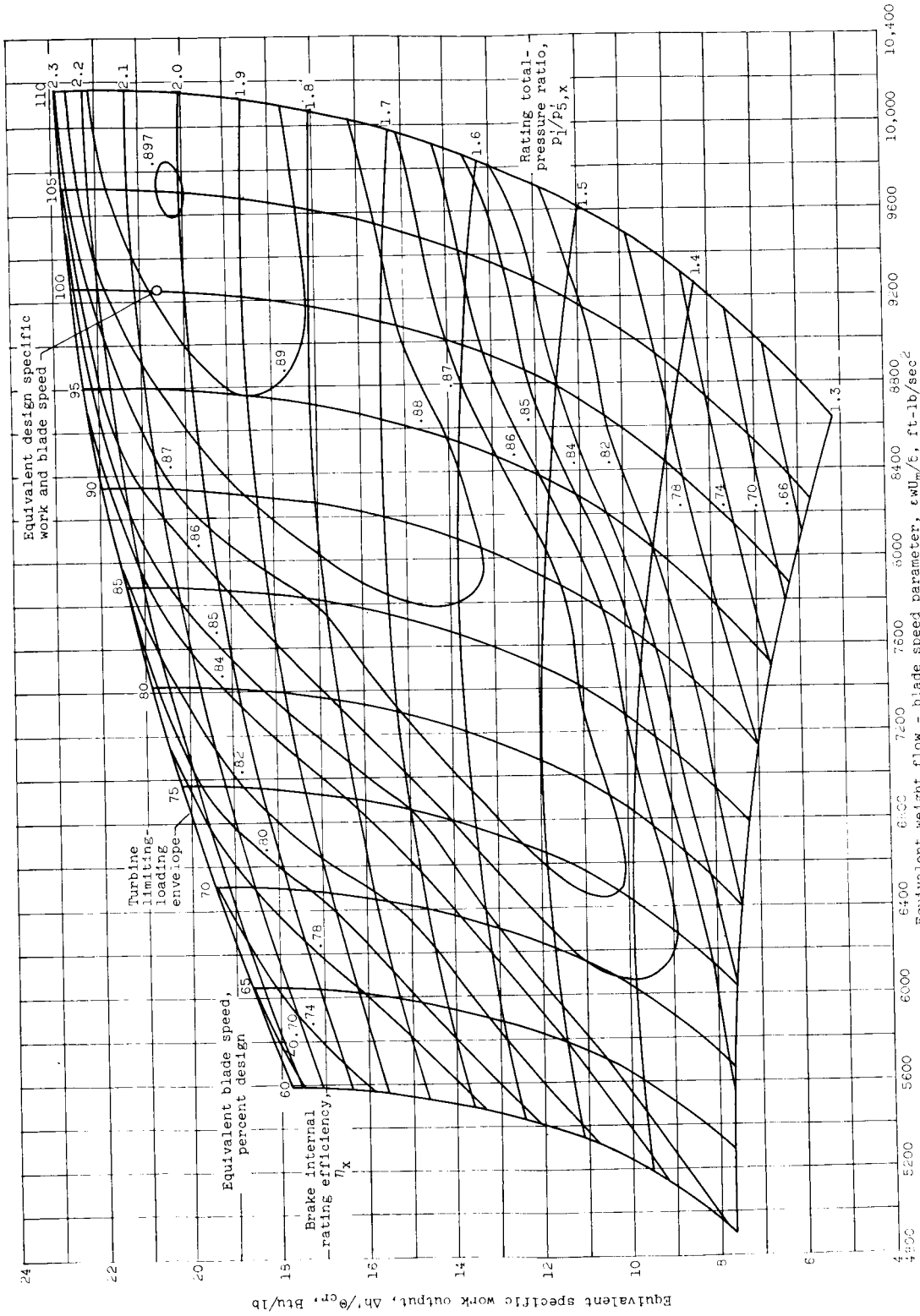




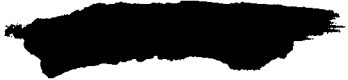
(a) Based on actual total-pressure ratio across turbine.

Figure 5. - Experimentally obtained turbine performance maps.





(b) Based on rating total-pressure ratio across turbine.
 Figure 5. - Concluded. Experimentally obtained turbine performance maps.



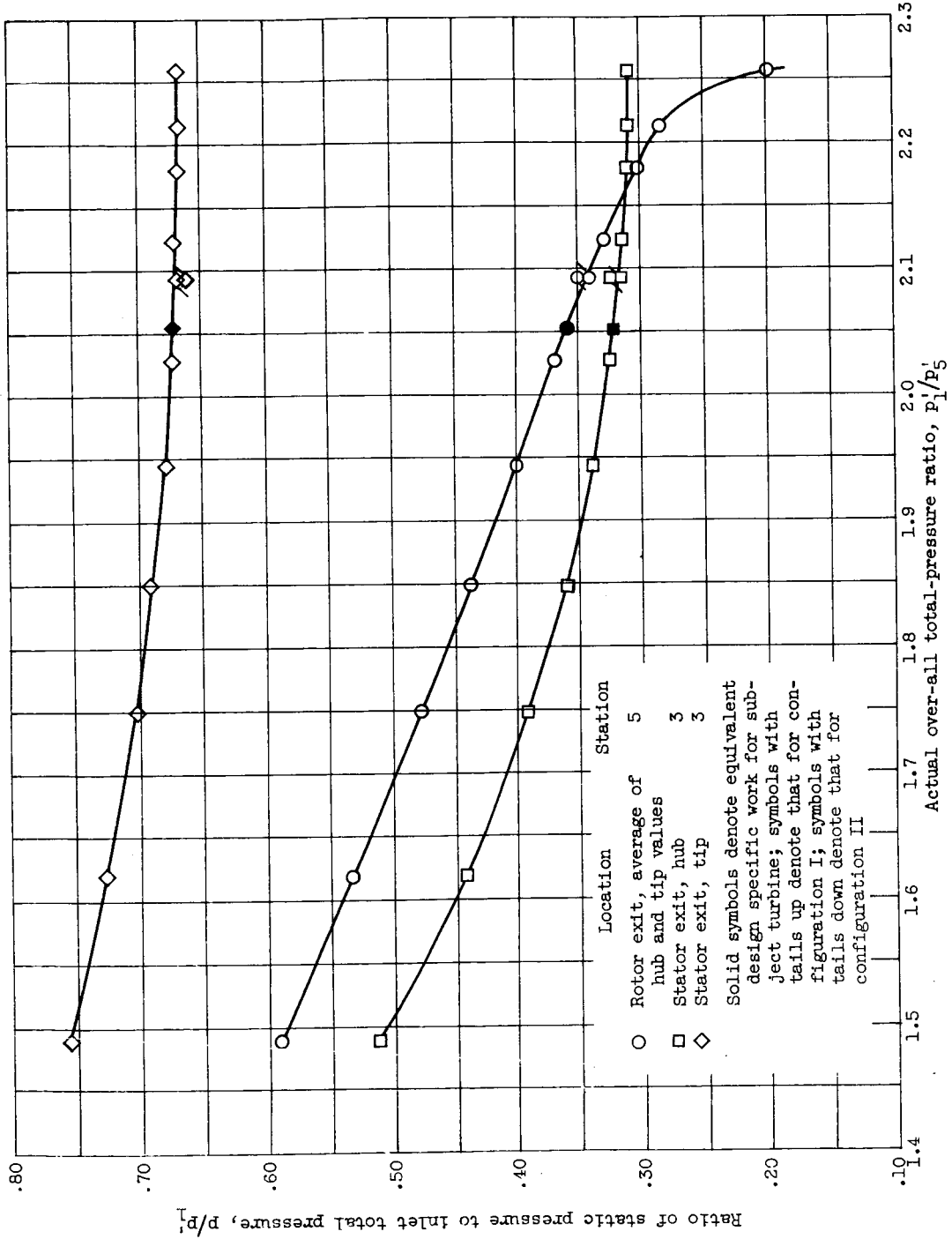
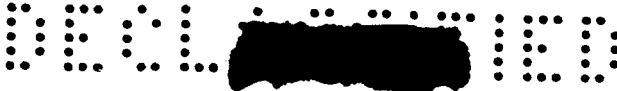


Figure 6. - Variation of static pressure behind stator and rotor with actual over-all total-pressure ratio at design speed.



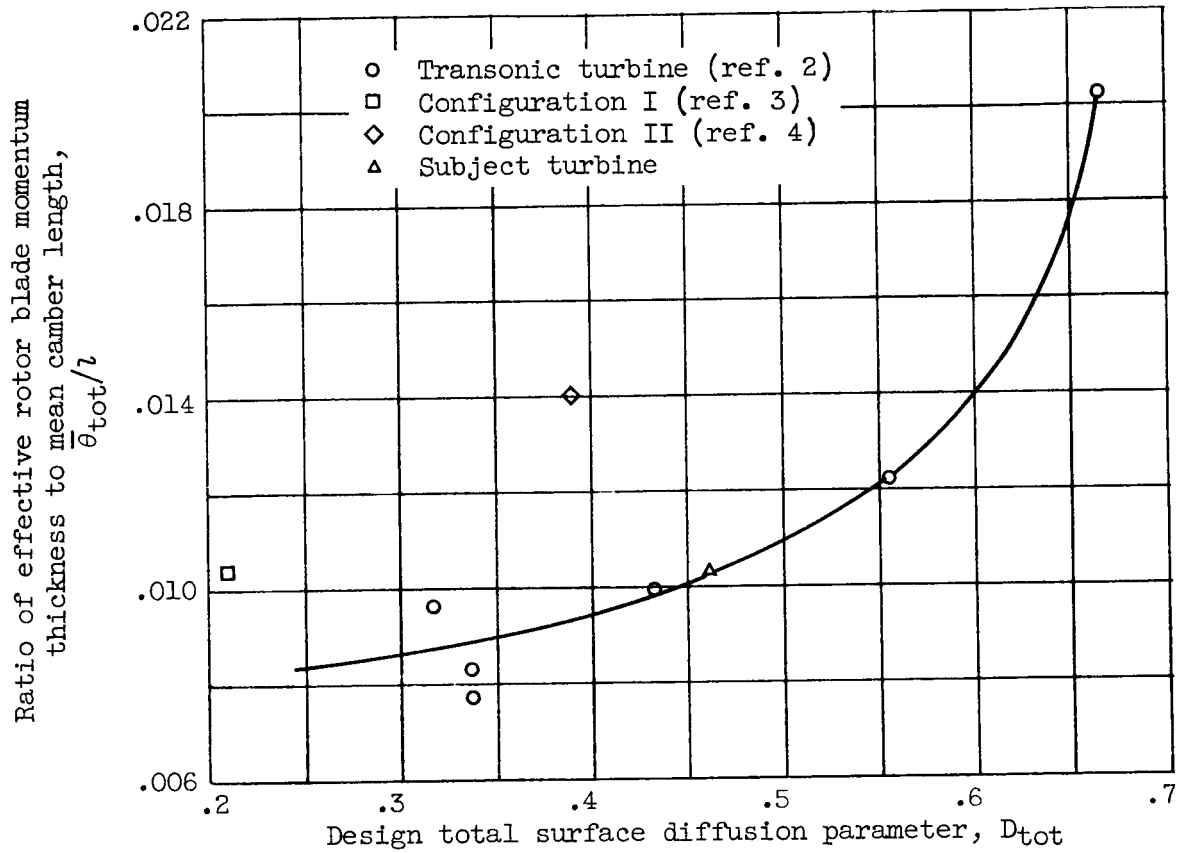


Figure 7. - Comparison of ratio of effective rotor blade momentum thickness to mean camber length of subject turbine with values for turbines of references 2, 3, and 4.

